# Thermal Treatment of 3D-printed Titanium Alloy

Michaela Fousova, Dalibor Vojtech
Department of Metals and Corrosion Engineering, University of Chemistry and Technology Prague. Technicka 5, 166 28 Prague. Czech Republic. E-mail: fousovam@vscht.cz

**In metals processing, 3D printing is a relatively new technology. It brings many advantages into production thanks to its additive principle on which it is based. One of the intended applications of 3D printing is especially regenerative medicine and aerospace industry that require products of very complex shapes. In these domains, titanium along with its alloys belongs among the most frequently used materials. When printing a Ti6Al4V alloy, very high cooling rates during the successive laser melting of an initial powder material result in high internal stresses. These stresses are followed with several problems, such as low material plasticity, possible cracking of built products, deformations of thin parts and similarly. Therefore, after the 3D printing process itself, a thermal treatment is applied to relief the stresses. The object of this study is to show the influence of atmosphere in thermal treatment process on the quality of final parts. The results show that oxygen absence is essential in terms of material plasticity.**

**Keywords:** 3D printing, Titanium, Thermal treatment

## 1 Introduction

3D printing brings many advantages into production; especially geometry freedom provided by the additive way of manufacture (based on which 3D printing is called additive manufacture too). Such advantage is very appreciated by industrial manufactures producing parts of complex shapes which production is very demanding, time-consuming and costly. By implementation of 3D printing, production steps are significantly reduced and so is a material waste because parts can be printed in the near-net shape exactly according to a 3D computer model by joining input material (in the form of powders or wires) together [1,2,3].

Nevertheless, 3D printing has also its issues as everything does. There are many process parameters entering the production process that must be optimized for each material and even for different products of the same material to achieve the required quality. Thanks to a huge interest in this modern technology, there have been many studies and a wide range of materials can be already successfully processed [4,5]. For metals, selective melting of powder materials by laser or electron beam is mostly applied (SLM and EBM technologies) [6]. With these technologies, rapid melting and subsequent cooling are coupled, what brings high internal stresses into products, formation of metastable microstructures, segregation and other specific features. These phenomena may yield in part distortion, deformation, cracking, undesirable properties etc. Therefore, different approaches are used to limit the undesired issues [7,8].

Titanium and its alloys belong among the most applied materials in the field of high-demanding products. When processing by 3D printing, the as-printed parts suffer from high internal stresses and metastable martensitic microstructure, both connected with a low plasticity. From this reason, a thermal treatment is recommended [9].

This work was done in cooperation with an industrial producer of 3D-printed medical implants. This producer encountered problems with a variable part quality after a heat treatment provided by an external supplier. Therefore, the aim of our work was to reveal the problem and to study the influence of atmosphere present in heat treatment process. In this paper, three possible atmospheres are shown and their influence on material surface, chemical composition and mechanical properties is characterized and compared with the as-built state.

## 2 Materials and Methods

### 2.1 3D printing

Specimens of a Ti6Al4V alloy were prepared by means of the selective laser melting (SLM) technology which belongs into the group of powder-bed techniques of 3D printing. In case of deeper interest in the SLM technology, please see our previous paper [10] where a detail description is given. M2 Cusing machine equipped with one Yb:YAG laser of 200 W power (ConceptLaser, Germany) was used. A gas-atomized powder of the Ti6Al4V alloy (rematitan® CL, Dentaurum) with particles size in the range of 15-45 μm served as the process input. The process of laser melting of the powder material was carried out in a work chamber supplied with an argon atmosphere (technical argon of 4.6 purity). The building platform, on which layers of powder of 30 μm in thickness were deposited, was preheated to 200 °C. Laser beam was scanned across the powder bed with a scanning speed of 1250 mm/s and a laser power of 200 W. The hatching distance between adjacent scan tracks was set to 80 μm. An island scanning strategy and a continuous regime were applied. Specimens were printed directly in the shape required for tensile testing (CSN EN ISO 6892-1).

### 2.2 Thermal treatment

The aim of this work was to study the influence of atmosphere present in thermal treatment process on part quality (surface state, chemical composition, mechanical properties). The regime of the thermal treatment was based on a commercially proposed one. The commercially used regime consists in annealing the 3D-printed parts at the temperature of 820 °C for 90 minutes under a

protective argon atmosphere. The parts are heated up in the furnace with a heating rate set to 200 °C/h and, after the treatment, cooled down slowly to 500 °C, then removed and air-cooled to room temperature.

The first series of specimens was thermally treated under a vacuum ($10^{-5}$ mbar) in a vertical vacuum furnace (Xerion XRETORT). The removal of the specimens was not possible at 500 °C, so that the specimens were furnace-cooled down to 100 °C. The second series was treated under an argon atmosphere in an electric muffle furnace Svoboda 018 ZP 80. A technical argon ($O_2$ content <5 ppm) was supplied continuously into a graphite form in which the specimens were covered in fine titanium machined-turnings. Such an arrangement was intended to prevent oxidation by preferential oxidation of the titanium getter. The last series of thermal treatment was carried out in a muffle furnace Martinek MP 05 without any protective atmosphere.

### 2.3 Characterization of thermally treated samples

All the thermally treated specimens were characterized in terms of surface oxidation, changes in chemical composition and mechanical properties. Specimens in the as-built condition served as a reference.

Metallographic cross-sections were prepared by a standard metallographic way, polished and etched in Kroll's reagent to reveal microstructure. The microstructure was observed using scanning electron microscopy (abbr. SEM, TESCAN VEGA-3 LMU) equipped with energy-dispersive spectroscopy analyser (abbr. EDS, INCA 350). The thickness of oxide layers formed on the surface was assessed by image analysis in ImageJ software. The phase composition of the oxide layers was determined by X-ray diffraction analysis (abbr. XRD, PANalytical X'Pert PRO with Cu anode).

To determine how and to what extent the chemical composition of the alloy had been affected by the thermal treatment, wavelength-dispersive spectroscopy (abbr. WDS) was applied and depth profiles were constructed. Also hardness depth profile was measured using a microhardness tester Future-Tech FM-700 (CSN EN ISO 6507). A Vickers indentor with the load of 50 g (HV0.05) applied for 10 s was used.

The overall impact of the atmosphere in the heat treatment process on the specimens performance was represented by tensile tests (CSN EN ISO 6892-1). The tensile tests were performed on three specimens of each series at a strain rate of 0.001 $s^{-1}$ using a universal testing machine LabTest 5.250SP1-VM.

## 3 Results and discussion

### 3.1 Surface oxidation and affection of a surface layer of the alloy

After the thermal treatment, an oxide layer was formed on the specimens surface. The layers can be seen in **Fig. 1**. In vacuum, almost no layer was observed. The thickness of the layer formed in the argon atmosphere was determined to be 0.3±0.1 μm. The thickest layer covered the surface of specimens treated in air, with thickness being 9.0±4.5 μm.

The XRD analysis revealed that the oxide layer is composed of $TiO_2$ (rutile), $Al_2O_3$ (corundum) and a minor amount of $V_2O_5$. Because of the higher affinity of aluminium to oxygen compared to titanium, aluminium is oxidized first. Therefore, $Al_2O_3$ forms an upper part of the oxide layer. That is clearly illustrated by elemental maps in **Fig. 2** obtained by EDS analysis showing distribution of elements within the oxide layer formed on the surface of a specimen heat treated in air. Considering the application in the human body, previous research stated that these oxides are favourable for the growth of bone cells [11,12]. However, in this case, the adhesion of the oxide layers is questionable. Especially, the oxide layer on the surface of the series of specimens treated in air was already so thick that it cracked at multiple sites. During the real application, fragments which might release into the organism could already pose a health risk despite their cytocompatibility [13].

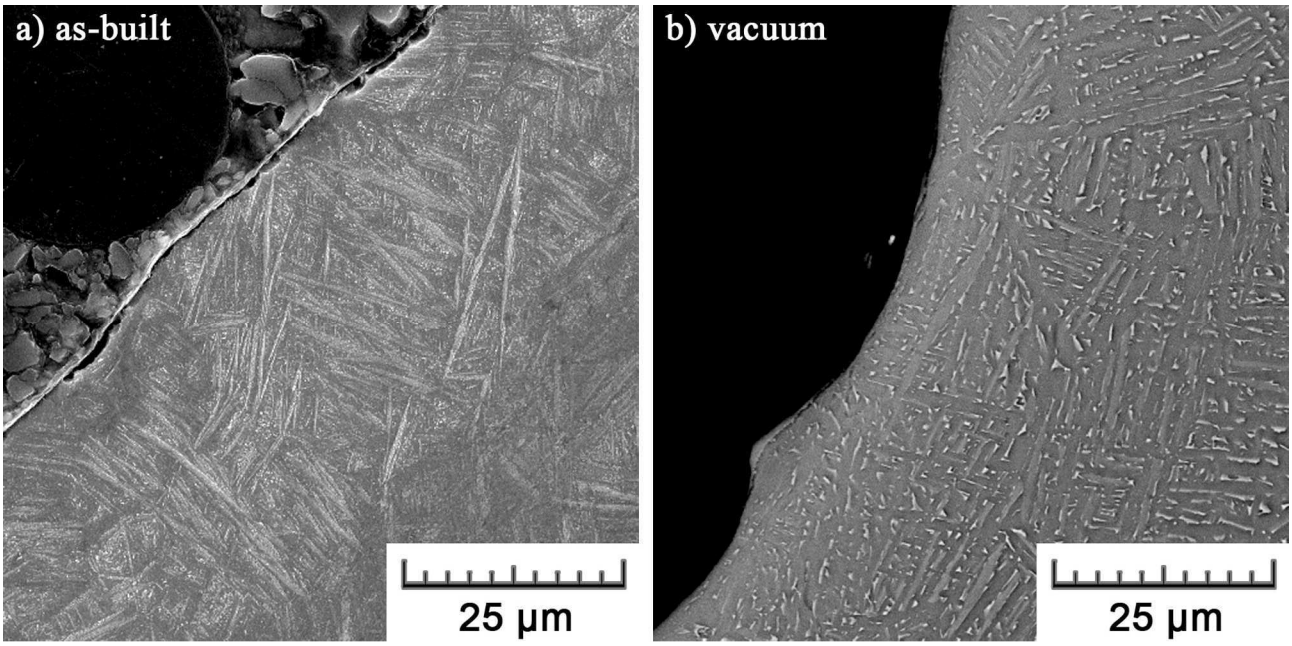

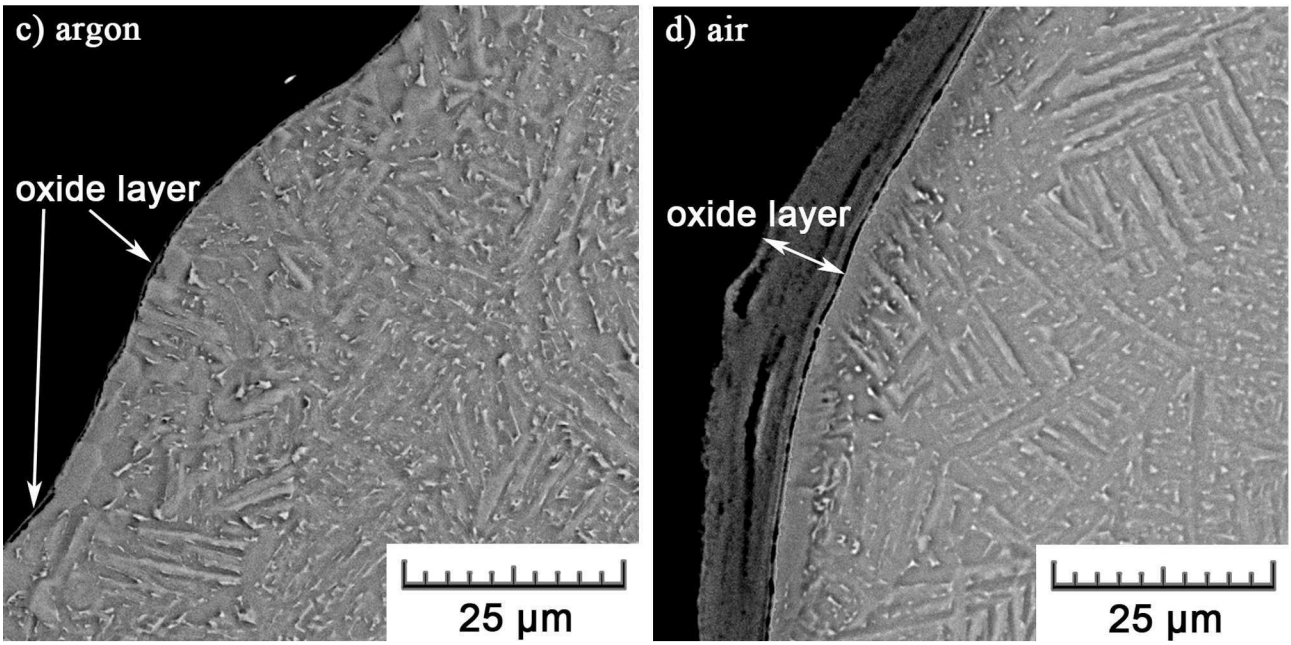


***Fig. 1*** *Micrographs and hardness profiles showing atmosphere influence*

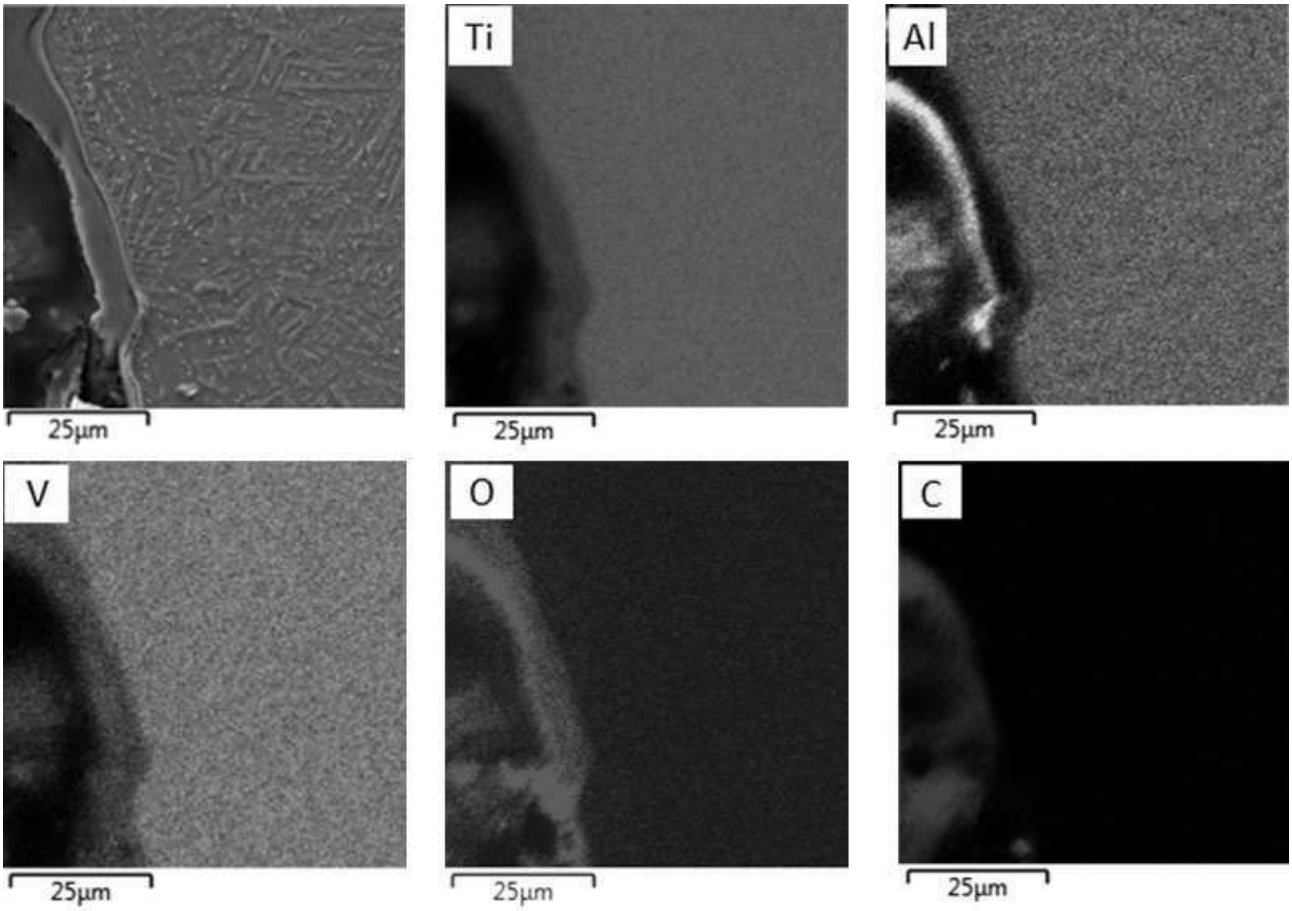


***Fig. 2*** *Micrographs showing atmosphere influence*

Regarding the microstructure, images in **Fig. 1** evidence changes after the heat treatment. In the as-built state (**Fig. 1a**), the microstructure fully consists of a metastable hcp martensite α´ phase. Martensitic diffusionless, shear-type transformations takes place due to high thermal gradients ($10^6$ °C/m) and very high cooling rates (up to $10^8$ °C/s) occurring during the laser melting process [14]. With respect to the temperature of the applied heat treatment (820 °C) higher than the temperature of martensite decomposition (600-650 °C), martensitic needles change into lamellae of α phase [15]. As martensite is enriched in vanadium being a β stabilizer, atoms of vanadium diffuse out of the newly formed α phase and β phase is formed in the interlamellar space consequently [16].

Despite coarsening of original martensitic needles, the microstructure remains very fine, with thickness of α-lamellae about 1 μm.

To determine the affection of the surface layer of the Ti6Al4V alloy by a particular atmosphere, depth profiles were constructed. The hardness measurement showed an affection of mechanical properties related to changes in the chemical composition, while the WDS analysis provided information about the chemical composition directly. The hardness profiles are shown in **Table 1**. No hardening was registered in the as-built state neither in the vacuum heat treated state. Conversely, hardening of a surface layer is clear in the series heat treated in argon and air. Data showing the affected depth of the material and the maximum hardness are given in **Table 2**. The strongest hardening was detected in air series, with maximum hardness of 640.1 HV0.05 signifying an increase from the average hardness by 85%. A layer of 60 μm was affected. WDS showed a corresponding profile of oxygen concentration. The maximum concentration reached 8.1 wt.%. Therefore, the hardening can be explained by incorporation of oxygen atoms into the interstitial positions of the α solid solution. Although only a very thin oxide layer was formed on the surface after the heat treatment in argon, the material itself was also affected. The reasons may be following: 1. Owing to the use of technical argon, there were oxygen residues. 2. Because the used furnace was not a hermetically sealed furnace, there might have been air leakages. 3. The 'gettering' capacity of the used titanium turnings was probably insufficient. A fine titanium powder would be suitable for this purpose, but at the expense of significantly higher costs. Even so, the hardness profile c) in **Tab. 1** indicates a notably lower affection than in the air. The maximum O concentration detected by WDS was 3.6 wt.%.

***Tab. 1*** *Hardness profiles showing atmosphere influence: a) as-built, b) vacuum, c) argon, d) air*

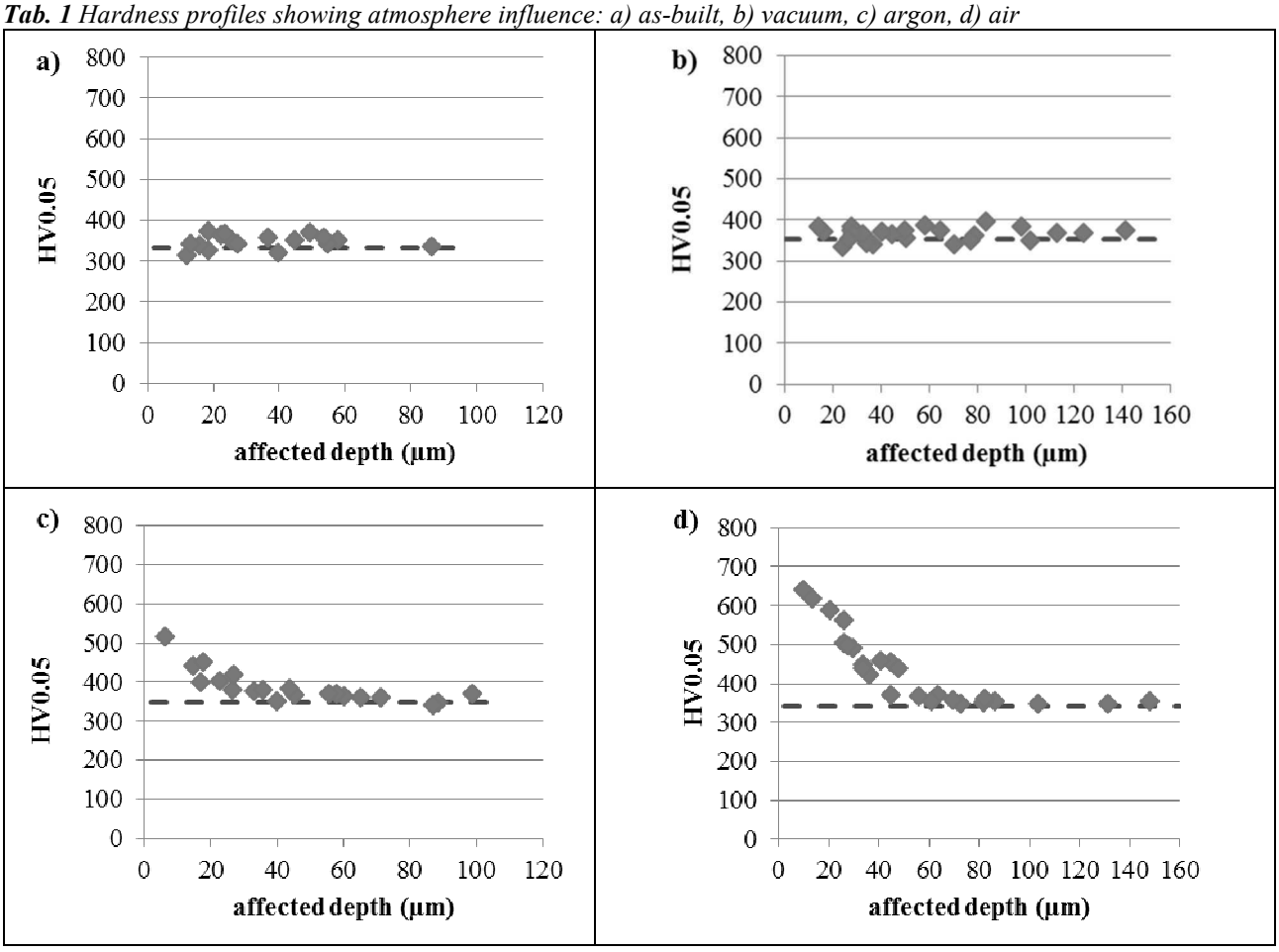


***Tab. 2*** *Affected depth and hardening caused by oxygen*

| | Affected depth (μm) | Max. hardness (HV0.05) | Material hardness (HV0.05) |
|---|---|---|---|
| **as-built** | - | 373.8 | 352.2±5.5 |
| **vacuum** | - | 396.9 | 352.9±2.6 |
| **argon** | 45 | 517.5 | 352.1±5.1 |
| **air** | 60 | 640.1 | 345.3±5.1 |

### 3.2 Mechanical properties

To show how the different atmospheres and related oxygen affection had influenced the mechanical performance of the specimens, tensile tests were carried out. **Figure 3** shows representative stress-strain curves for every series. Average values of tensile yield strength

(TYS), ultimate tensile strength (UTS) and elongation (A) are summarized in **Table 3**.

Thanks to the very fine martensitic microstructure (**Fig. 1a**), TYS and UTS are the highest for the as-built state. However, the metastable martensitic microstructure along with high internal stresses originating from rapid solidification in the building process are both reasons of a low plasticity. The elongation reached only 4.3±1.5%, which is a value that do not meet the requirements posed on implants (10%). Because of that, a thermal treatment is always recommended.

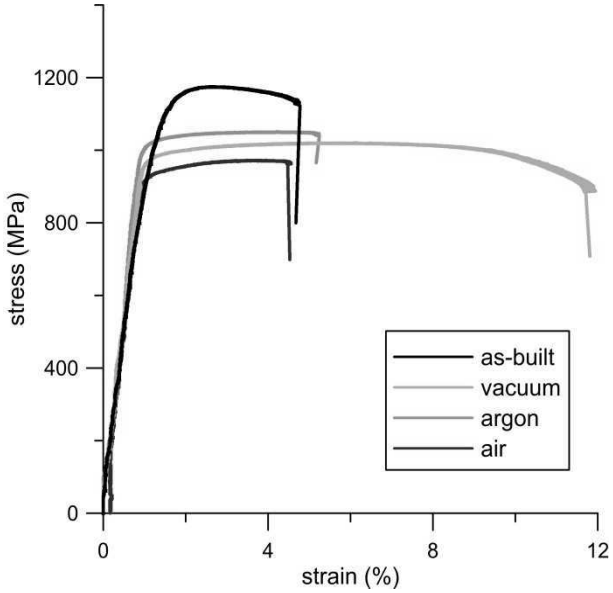


***Fig. 3*** *Representative tensile stress-strain curves*

***Tab. 3*** *Mechanical properties of specimens heat treated in different atmospheres*

| | TYS (MPa) | UTS (MPa) | A (%) |
|---|---|---|---|
| **as-built** | 1000±21 | 1193±35 | 4.3±1.5 |
| **vacuum** | 973±4 | 1023±4 | 9.0±2.0 |
| **argon** | 996±19 | 1040±9 | 3.8±0.4 |
| **air** | 937±24 | 980±24 | 3.7±1.5 |

As the micrographs in **Fig. 1** show, the microstructure changed to two-phase lamellar one after all the thermal treatments. At the temperature of 820 °C, the martensitic needles decomposed into a mixture of α+β lamellae. Also, the internal stresses were relieved. Therefore, a drop in TYS and UTS was registered in all the cases. The elongation increased only in the case of vacuum where no oxidation occurred. There, the value of 9.0±2.0% already approaches the desired milestone of 10%. In argon and air, the elongation even fell slightly below the original value in the as-built condition. The drop in material plasticity may be attributed to fragile layers of oxides covering the surface (**Fig. 1c,d**) and to the affection of a surface layer (to the depth of ~ 50 μm) by oxygen. The fragile oxides facilitate crack initiation. Oxygen atoms that diffused into the alloy contribute to the solid solution hardening and simultaneously impair elongation by blocking dislocation motion.

A comparison of fracture surfaces shown in **Fig. 4** illustrates the above-stated detected features. In the as-built condition, the fracture surface showed a ductile nature characterized by a fracture morphology with fine dimples. Such a morphology was present globally across the whole fracture surface (**Fig. 4a**). After the heat treatment in vacuum, the same was observed. Conversely, the oxygen affection was manifested on fracture surfaces of specimens heat treated in argon and air. The surface layer showed clearly brittle nature compared to the rest of the fracture surface (**Fig. 4b**). The thickness of this brittle layer corresponds to the determined depth of the material affected by oxygen (**Table 1**).

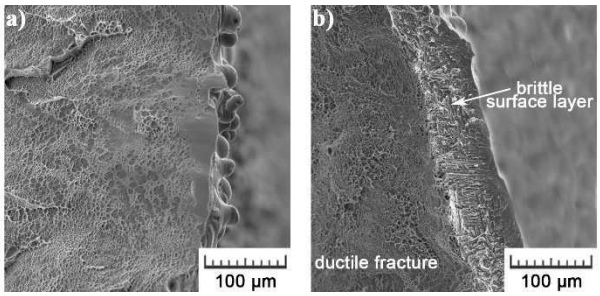


***Fig. 4*** *Comparison of fracture surfaces: a) as-built, b) heat treated - air*

## 4 Conclusion

In this work, the influence of atmosphere applied in the heat treatment process was studied. The study showed that oxygen has a strongly negative effect, even if present in minor amount (e.g. in technical argon). Oxide layers are formed on the specimens surface and oxygen atoms diffuse into the material, what leads to the hardening by interstitial solid solution and decrease in elongation. The desired increase in elongation was obtained only in vacuum. Since the thickness of the affected layer of the material was 60 μm in the worst case, it could be machined to achieve the desired properties. However, this is only possible for simple compact components. For porous structures and for the preparation of parts in the final form, it is necessary to carry the heat treatment out in vacuum or in high purity argon.

## Acknowledgement

***The authors wish to thank the Czech Science Foundation (project no. P108/12/G043) for the financial support of this research.***

## References

[1] FORD, S., DESPEISSE, M. (2016). Additive manufacturing and sustainability: an exploratory study of the advantages and challenges. *Journal of Cleaner Production*, 2016, Vol. 137, Supplement C, pp. 1573-1587.

[2] SUN, Z., TAN, X., TOR, S. B., YEONG, W. Y. (2016). Selective laser melting of stainless steel 316L with low porosity and high build rates. *Materials & Design*, 2016, Vol. 104, pp. 197-204.

[3] HANZL, P., ZETKOVÁ, I., ZETEK, M. (2017). Load Capacity of a Gyroid Structure Produced by Selective Laser Melting. *Manufacturing Technology*, 2017, Vol. 17, No. 5, pp. 459-463

[4] MURR, L. E., MARTINEZ, E., AMATO, K. N., GAYTAN, S. M., HERNANDEZ, J., RAMIREZ, D. A., SHINDO, P. W., MEDINA, F., WICKER, R. B. (2012). Fabrication of Metal and Alloy Components by Additive Manufacturing: Examples of 3D Materials Science. *Journal of Materials Research and Technology*, 2012, Vol. 1, No. 1, pp. 42-54.

[5] HANZL, P., ZETEK, M., BAKŠA, T., KROUPA, T. (2015). The Influence of Processing Parameters on the Mechanical Properties of SLM Parts. *Procedia Engineering*, 2015, Vol. 100, pp. 1405-1413.

[6] MURR, L. E., GAYTAN, S. M., RAMIREZ, D. A., MARTINEZ, E., HERNANDEZ, J., AMATO, K. N., SHINDO, P. W., MEDINA, F. R., WICKER, R. B. (2012). Metal Fabrication by Additive Manufacturing Using Laser and Electron Beam Melting Technologies. *Journal of Materials Science & Technology*, 2012, Vol. 28, No. 1, pp. 1-14.

[7] HERZOG, D., SEYDA, V., WYCISK, E., EMMELMANN, C. (2016). Additive manufacturing of metals. *Acta Materialia*, 2016, Vol. 117, pp. 371-392.

[8] PARRY, L., ASHCROFT, I. A., WILDMAN, R. D. (2016). Understanding the effect of laser scan strategy on residual stress in selective laser melting through thermo-mechanical simulation. *Additive Manufacturing*, 2016, Vol. 12, Part A, pp. 1-15.

[9] VRANCKEN, B., THIJS, L., KRUTH, J.-P., VAN HUMBEECK, J. (2012). Heat treatment of Ti6Al4V produced by Selective Laser Melting: Microstructure and mechanical properties. *Journal of Alloys and Compounds*, 2012, Vol. 541, pp. 177-185.

[10] FOUSOVÁ, M., VOJTĚCH, D., KUBÁSEK, J. (2016). Titanium alloy Ti-6Al-4V prepared by Selective Laser Melting (SLM). *Manufacturing Technology*, 2016, Vol. 16, No. 4, pp. 691-697.

[11] FOUSOVÁ, M., VOJTĚCH, D., KUBÁSEK, J., JABLONSKÁ, E., FOJT, J. (2017). Promising characteristics of gradient porosity Ti-6Al-4V alloy prepared by SLM process. *Journal of the Mechanical Behavior of Biomedical Materials*, 2017, Vol. 69, pp. 368-376.

[12] WANG, M., WU, Y., LU, S., CHEN, T., ZHAO, Y., CHEN, H., TANG, Z. (2016). Fabrication and characterization of selective laser melting printed Ti–6Al–4V alloys subjected to heat treatment for customized implants design. *Progress in Natural Science: Materials International*, 2016, Vol. 26, No. 6, pp. 671-677.

[13] BITAR, D., PARVIZI, J. (2015). Biological response to prosthetic debris. *World Journal of Orthopedics*, 2015, Vol. 6, No. 2, pp. 172-189.

[14] YANG, J., YU, H., YIN, J., GAO, M., WANG, Z., ZENG, X. (2016). Formation and control of martensite in Ti-6Al-4V alloy produced by selective laser melting. *Materials & Design*, 2016, Vol. 108, Supplement C, pp. 308-318.

[15] ALI, H., MA, L., GHADBEIGI, H., MUMTAZ, K. (2017). In-situ residual stress reduction, martensitic decomposition and mechanical properties enhancement through high temperature powder bed pre-heating of Selective Laser Melted Ti6Al4V. *Materials Science and Engineering*: A, 2017, Vol. 695, Supplement C, pp. 211-220.

[16] SALLICA-LEVA, E., CARAM, R., JARDINI, A. L., FOGAGNOLO, J. B. (2016). Ductility improvement due to martensite α′ decomposition in porous Ti–6Al–4V parts produced by selective laser melting for orthopedic implants. *Journal of the Mechanical Behavior of Biomedical Materials*, 2016, Vol. 54, pp. 149-158.

**10.21062/ujep/82.2018/a/1213-2489/MT/18/2/227**